

Pseudo-Spin, Real-Spin and Spin Polarization of Photo-emitted Electrons

Rui Yu¹, Hongming Weng^{2,3}, Zhong Fang^{2,3}, Xi Dai^{2,3*}

¹ *Department of Physics, Harbin Institute of Technology, Harbin 150001, China*

² *Beijing National Laboratory for Condensed Matter Physics, and Institute of Physics, Chinese Academy of Sciences, Beijing 100190, China and*

³ *Collaborative Innovation Center of Quantum Matter, Beijing 100190, China*

(Dated: March 27, 2022)

In this work, we discuss the connections between pseudo spin, real spin of electrons in material and spin polarization of photo-emitted electrons out of material. By investigating these three spin textures for Bi₂Se₃ and SmB₆ compounds, we find that the spin orientation of photo-electrons for SmB₆ has different correspondence to pseudo spin and real spin compare to Bi₂Se₃, due to the different symmetry properties of the photo-emission matrix between initial and final states. We calculate the spin polarization and circular dichroism spectra of photo-emitted electrons for both compounds, which can be detected by spin-resolved and circular dichroism angle resolved photo-emission spectroscopy experiment.

I. INTRODUCTION

The experimental technique of angle resolved photo-emission spectroscopy (ARPES) is a powerful tool in investigating the electronic structure of crystalline materials. The energy and momentum information of the electrons inside a materials can be obtained by measuring the kinetic energy and angular distribution of the photo-emitted electrons from a sample illuminated with sufficiently high-energy radiation. To detect the spin information of the electronic states, the spin-resolved ARPES and circular dichroism (CD) ARPES have been recently widely used in revealing the novel spin and orbital texture of the topological surface states of three-dimensional topological insulators^{1,2}.

The spin-resolved ARPES for surface states of Bi₂Se₃ family of topological insulator materials have been well studied theoretically and experimentally in recent years, which show that the spin orientation of photo-electrons can be completely different from their initial states and strongly depends on the polarization of the incident light³⁻¹⁰. These results reveals that three different definition of the spin texture for the topological surface states, namely the pseudo spin and real spin orientation for electronic states inside the crystal and that of the photo-emitted electrons in the vacuum, which are often mentioned within the context of spin resolved ARPES experiments, are indeed very different and should be clarified rigorously and studied separately^{5,9}. In the present paper, by comparing the above mentioned three different type of “spin texture” for the surface states of two well known topological insulators, Bi₂Se₃ and SmB₆, we reveal that how these three concepts are related to each other.

The rest of the paper is organized as follows. In section II, we give the formulas for the pseudo spin, the real spin of electrons in materials and the spin polarization of photo-electrons in the ARPES measurement. Then we discuss the pseudo spin texture, the real spin texture and the spin-resolved and CD spectra ARPES for Bi₂Se₃ (111) surface states in section III and for SmB₆ (001)

surface states in section IV. Conclusions are given in the end of this paper.

II. THREE DIFFERENT DEFINITION OF “SPIN TEXTURE”

In general, the topological surface states can be described by a 2×2 Dirac Hamiltonian

$$H(\mathbf{k}) = d_0(\mathbf{k})\sigma_0 + d_x(\mathbf{k})\sigma_x + d_y(\mathbf{k})\sigma_y + d_z(\mathbf{k})\sigma_z, \quad (1)$$

where σ_0 is identity matrix and $\sigma_{x,y,z}$ are Pauli matrices indicating the space expanded by the eigenfunction φ_{\pm} at the Dirac point. φ_{\pm} form Kramers doublet at the time-reversal symmetry point $\mathbf{k} = 0$ and we denote them as pseudo spin in the following text. The pseudo spin texture can be obtained by calculating the expected value of $\boldsymbol{\sigma}$ matrix as

$$\langle \boldsymbol{\sigma} \rangle_{\mathbf{k}} = (\langle \mathbf{k} | \sigma_x | \mathbf{k} \rangle, \langle \mathbf{k} | \sigma_y | \mathbf{k} \rangle, \langle \mathbf{k} | \sigma_z | \mathbf{k} \rangle), \quad (2)$$

where $|\mathbf{k}\rangle$ is the eigenstates of Eq. (1).

In order to get the real spin vector on the surface states, one need to know the real spin operator \mathbf{s} for the surface states. The connection between real spin operator \mathbf{s} and pseudo spin operators $\boldsymbol{\sigma}$ are characterized by the following “g-factor” matrix

$$(s_x, s_y, s_z) = (\sigma_x, \sigma_y, \sigma_z) \begin{bmatrix} g_{xx} & g_{xy} & g_{xz} \\ g_{yx} & g_{yy} & g_{yz} \\ g_{zx} & g_{zy} & g_{zz} \end{bmatrix}. \quad (3)$$

This “g-factor” matrix can be obtained by projecting the real spin operators into the surface states subspace φ_{\pm} ¹¹. After obtaining \mathbf{s} , one can get the expectation value of real spin for any electronic state with momentum \mathbf{k} as

$$\langle \mathbf{s} \rangle_{\mathbf{k}} = (\langle \mathbf{k} | s_x | \mathbf{k} \rangle, \langle \mathbf{k} | s_y | \mathbf{k} \rangle, \langle \mathbf{k} | s_z | \mathbf{k} \rangle). \quad (4)$$

Before discussing the spin polarization of photo-electrons, we first give some formulas for calculating the photo-emission final states. We start from a microscopic

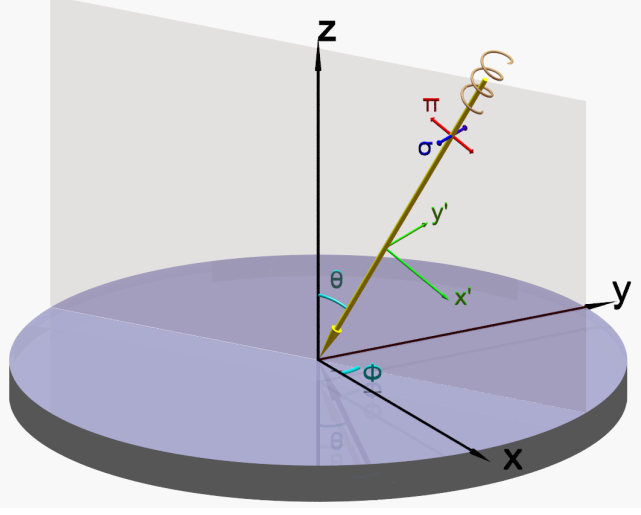


Figure 1. Diagram of the experimental geometry. Linear polarization (σ -polarized and π -polarized) and circular polarization (right and left circular polarized) of photons can be continuously rotated by θ and ϕ angle as shown in the figure.

Hamiltonian for a system with spin-orbit coupling, which reads

$$H = \frac{\mathbf{p}^2}{2m} + V(\mathbf{r}) + \frac{\hbar}{4m^2c^2} \mathbf{p} \times \nabla V \cdot \mathbf{s}, \quad (5)$$

where \mathbf{p} is momentum operator, $V(\mathbf{r})$ is crystal potential and \mathbf{s} is electron spin operator. The Hamiltonian for system coupling to an electromagnetic field is obtained via the Peierls substitution $\mathbf{p} \rightarrow \mathbf{p} - e\mathbf{A}$, where \mathbf{A} is the vector potential for the incident light. The linear and circular polarized incident light are schematically shown in Fig. 1 and their formulas are given in appendix A. The electron-photon interaction term can then be obtained as

$$\begin{aligned} H_{int} &= H(\mathbf{p} - e\mathbf{A}) - H = -\mathbf{A} \cdot \mathcal{P} \\ &= -\left[\frac{1}{2}(A_- \mathcal{P}_+ + A_+ \mathcal{P}_-) + A_z \mathcal{P}_z \right], \end{aligned} \quad (6)$$

where $\mathcal{P} = \frac{e}{m} \mathbf{p} - \frac{\hbar}{4m^2c^2} \nabla V \times \mathbf{s}$, $\mathcal{P}_{\pm} = \mathcal{P}_x \pm i\mathcal{P}_y$ and $A_{\pm} = A_x \pm iA_y$.

The photo-emitted final states can be expressed as

$$|f\rangle = \sum_{\alpha=\uparrow,\downarrow} |f_{\alpha}\rangle \langle f_{\alpha}| \mathcal{A} \cdot \mathcal{P} |k\rangle \quad (7)$$

where $|f_{\alpha}\rangle$ are basis functions for final states with spin $\alpha = \uparrow, \downarrow$ and \mathcal{A} is the Fourier transform of \mathbf{A} . The spin polarization for $|f\rangle$ states can be calculated as

$$\langle \boldsymbol{\tau} \rangle_f = (\langle f | \tau_x | f \rangle, \langle f | \tau_y | f \rangle, \langle f | \tau_z | f \rangle), \quad (8)$$

where $\tau_{x,y,z}$ are Pauli matrices defined in $|f_{\uparrow}\rangle$ and $|f_{\downarrow}\rangle$ space. As expressed in Eq. (7) and Eq. (8), the spin polarization of photo-electrons are related to the matrix elements $\langle f_{\alpha} | \mathcal{A} \cdot \mathcal{P} | k \rangle$, which can be determined by considering the symmetry properties of the vector potential

\mathcal{A} and the initial states $|k\rangle$. In the following two section, we will discuss theoretically the spin polarization of the photo-emitted final states for Bi_2Se_3 and SmB_6 surface states with different types of polarized incident light, which can be measured from spin-resolved and CD ARPES experiment.

III. SPIN-RESOLVED AND CD ARPES FOR Bi_2Se_3 SURFACE STATES

For Bi_2Se_3 family of materials with surface terminated in (111) direction, a Dirac-like surface states exist at the $\bar{\Gamma}$ point in the surface Brillouin zone¹²⁻¹⁵. A 2×2 k-p model Hamiltonian, in basis of φ_{\pm} , preserving time-reversal and C_{3v} crystalline symmetry has been derived to describe these surface states. By considering the C_3 rotation symmetry, the basis functions φ_{\pm} can be classified into two classes, namely $j_z = \pm 1/2$ and $j_z = \pm 3/2$ classes. Other states with higher j_z values can be reduced into $j_z = \pm 1/2$ or $j_z = \pm 3/2$ classes by modulating 3 because of the discrete C_3 rotation symmetry in crystal. The first-principles calculations for Bi_2Se_3 show that the pseudo spin states φ_{\pm} transform as vectors with angular momentum $j_z = \pm 1/2$ and the model Hamiltonian for the Bi_2Se_3 (111) surface states takes the following Dirac-type formula

$$H = \hbar v(k_y \sigma_x - k_x \sigma_y) = \hbar v k (\sin \beta \sigma_x - \cos \beta \sigma_y) \quad (9)$$

in basis of $\{|j_z = +\frac{1}{2}\rangle, |j_z = -\frac{1}{2}\rangle\}$, where β is the angle between \mathbf{k} and the $+\vec{k}_x$ direction and $\sigma_{x,y}$ are the Pauli matrices in the pseudo spin space. The eigenvalues for above Hamiltonian are given as $E_{n,k} = n\hbar v k$, where $n = \pm 1$ indicate the eigenvalues above and below the Dirac cone. The Bloch periodic eigenstates are given as

$$|k\rangle_n = u_{nk} |+\frac{1}{2}\rangle + v_{nk} |-\frac{1}{2}\rangle = \frac{1}{\sqrt{2}} \begin{bmatrix} n i e^{-i\beta} \\ 1 \end{bmatrix}, \quad (10)$$

where $u_{nk} = n i e^{-i\beta} / \sqrt{2}$ and $v_{nk} = 1 / \sqrt{2}$. Using Eq. (2), the pseudo spin vectors can be calculated as

$$\langle \boldsymbol{\sigma} \rangle_{k,n} \propto n (\sin \beta, -\cos \beta, 0). \quad (11)$$

The spin operator \mathbf{s} is related to the pseudo spin operator $\boldsymbol{\sigma}$ as $(s_x, s_y, s_z) = (g_{xx} \sigma_x, g_{yy} \sigma_y, g_{zz} \sigma_z)$, whith $g_{xx,yy,zz}$ to be some constants¹¹. The real spin is proportional to the pseudo spin which can be calculated as

$$\langle \mathbf{s} \rangle_{k,n} \propto n (g_{xx} \sin \beta, -g_{yy} \cos \beta, 0) \quad (12)$$

as shown in Fig. 2.

Substitute Eq. (10) into Eq. (7), the photo-emitted

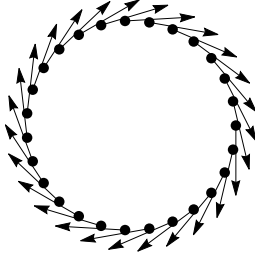


Figure 2. Real spin texture of Bi_2Se_3 (111) surface states with energy above the Dirac cone.

final states can be expressed as

$$\begin{aligned}
 |f\rangle \propto & \left| +\frac{1}{2} \right\rangle_{ff} \left\langle +\frac{1}{2} \right| \mathcal{A} \cdot \mathcal{P} \left| +\frac{1}{2} \right\rangle_i u_{nk} \\
 & + \left| +\frac{1}{2} \right\rangle_{ff} \left\langle +\frac{1}{2} \right| \mathcal{A} \cdot \mathcal{P} \left| -\frac{1}{2} \right\rangle_i v_{nk} \\
 & + \left| -\frac{1}{2} \right\rangle_{ff} \left\langle -\frac{1}{2} \right| \mathcal{A} \cdot \mathcal{P} \left| +\frac{1}{2} \right\rangle_i u_{nk} \\
 & + \left| -\frac{1}{2} \right\rangle_{ff} \left\langle -\frac{1}{2} \right| \mathcal{A} \cdot \mathcal{P} \left| -\frac{1}{2} \right\rangle_i v_{nk}. \quad (13)
 \end{aligned}$$

where the subscript i and f indicate the initial and final states respectively. The matrix elements in Eq. (13) can be determined by the symmetry considerations as discussed below.

At $\bar{\Gamma}$ point the symmetry is characterized by C_{3v} crystalline symmetry, which is reduced from space group $R\bar{3}m$ in the present of (111) direction surface and consists of a threefold rotation C_3 around z axis and a mirror operation $M_x: x \rightarrow -x$. Under these two operations, the basis functions are transformed as follows

$$M_x \left| \pm \frac{1}{2} \right\rangle_{i,f} = i \left| \mp \frac{1}{2} \right\rangle_{i,f}, \quad (14)$$

$$C_3 \left| \pm \frac{1}{2} \right\rangle_{i,f} = e^{-i\frac{2\pi}{3} \times (\pm\frac{1}{2})} \left| \pm \frac{1}{2} \right\rangle_{i,f}. \quad (15)$$

With the properties shown in Eq. (14) and Eq. (15), only the following four matrix elements in Eq. (13) are nonzero

$$f \left\langle +\frac{1}{2} \right| \mathcal{P}_+ \left| -\frac{1}{2} \right\rangle_i = -f \left\langle -\frac{1}{2} \right| \mathcal{P}_- \left| +\frac{1}{2} \right\rangle_i = a, \quad (16)$$

$$f \left\langle +\frac{1}{2} \right| \mathcal{P}_z \left| +\frac{1}{2} \right\rangle_i = f \left\langle -\frac{1}{2} \right| \mathcal{P}_z \left| -\frac{1}{2} \right\rangle_i = c, \quad (17)$$

where we used the property of $C_{3z} \mathcal{P}_\pm C_{3z}^\dagger = e^{\mp i\frac{2\pi}{3}} \mathcal{P}_\pm$ and a, c are complex parameters that should be determined from the first-principles calculations or by fitting with experimental results. With the help of Eq. (16) and Eq. (17), the final states $|f\rangle$ can thus be rewritten as

$$\begin{aligned}
 |f\rangle \propto & (av_{nk}\mathcal{A}_- + cu_{nk}\mathcal{A}_z) \left| +\frac{1}{2} \right\rangle_f \\
 & + (cv_{nk}\mathcal{A}_z - au_{nk}\mathcal{A}_+) \left| -\frac{1}{2} \right\rangle_f \\
 = & \frac{1}{\sqrt{2}} \begin{bmatrix} a\mathcal{A}_- + icne^{-i\beta}\mathcal{A}_z \\ -iane^{-i\beta}\mathcal{A}_+ + c\mathcal{A}_z \end{bmatrix}. \quad (18)
 \end{aligned}$$

The spin polarization of final states $|f\rangle$ can be calculated for light with different types of polarization.

(i) For σ -polarized light, $\mathcal{A}_\sigma = A_0(-\sin\phi, \cos\phi, 0)$, Eq. (18) takes the formula as

$$\begin{aligned}
 |f\rangle \propto & \frac{aA_0}{\sqrt{2}} \begin{bmatrix} -\sin\phi - icos\phi \\ -ine^{-i\beta}(-\sin\phi + icos\phi) \end{bmatrix} \\
 \propto & \frac{aA_0}{\sqrt{2}} \begin{bmatrix} 1 \\ ine^{-i(\beta-2\phi)} \end{bmatrix}. \quad (19)
 \end{aligned}$$

The spin polarization of final states $|f\rangle$ are calculated as

$$\langle \tau \rangle_f \propto n [\sin(\beta - 2\phi), \cos(\beta - 2\phi), 0]. \quad (20)$$

The spin polarization with different value of azimuth angle ϕ are shown in Fig. 3 and we set the energy of the initial states above the Dirac cone in the following text.

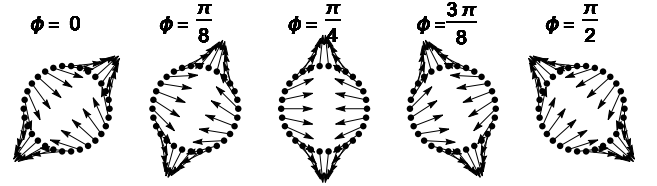


Figure 3. Spin polarization of photon-electrons with σ polarized light. Arrows indicate the spin directions in the xy plane.

(ii) For π -polarized light, we have $\mathcal{A}_\pi = A_0(\cos\theta\cos\phi, \cos\theta\sin\phi, -\sin\theta)$. Substitute \mathcal{A}_π into Eq. (18), we obtain the spin polarization of the photo-electrons as

$$\langle \tau_x \rangle_f = -2n|a|^2 \cos^2\theta \sin(\beta - 2\phi) + 2n|c|^2 \sin\beta \sin^2\theta - i(a^*c - ac^*) \sin 2\theta \sin\phi, \quad (21)$$

$$\langle \tau_y \rangle_f = -2n|a|^2 \cos^2\theta \cos(\beta - 2\phi) - 2n|c|^2 \cos\beta \sin^2\theta + i(a^*c - ac^*) \sin 2\theta \cos\phi, \quad (22)$$

$$\langle \tau_z \rangle_f = -n(a^*c + ac^*) \sin 2\theta \sin(\beta - \phi), \quad (23)$$

and the spin polarization textures with parameters $a = -0.9 + 0.1i$, $c = 0.5 - 0.1i$ with unit $\text{A} \cdot \text{m}$ are shown in Fig. 4.

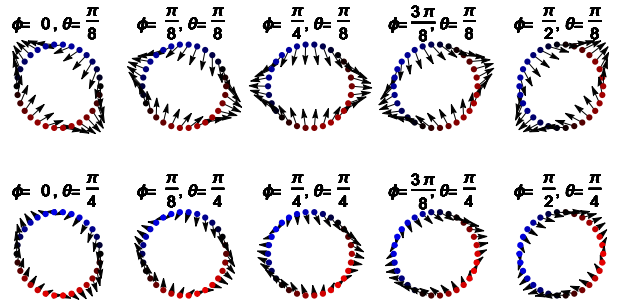


Figure 4. (Color online) Spin polarization of photon-electrons with π -polarized light. Arrows indicate the spin component in the xy plane. Color indicate the spin z component: red for $\langle \tau_z \rangle < 0$, blue for $\langle \tau_z \rangle > 0$ and black for $\langle \tau_z \rangle = 0$.

(iii) For circular polarized light, $\mathcal{A}_\eta = A_0(\cos\theta\cos\phi + \eta\sin\phi, \cos\theta\sin\phi - \eta\cos\phi, -\sin\theta)$, where $\eta = \pm 1$ are the index for right/left-handed circular polarized light. Substitute \mathcal{A}_η into Eq. (13), the spin polarization for photo-electrons are calculated as

$$\langle\tau_x\rangle_f = \sin\theta \left(-\eta(a^*c + ac^*)\cos\phi + i(a^*c - ac^*)\cos\theta\sin\phi + n|c|^2\sin\beta\sin\theta - n|a|^2\sin\theta\sin(2\phi - \beta) \right), \quad (24)$$

$$\langle\tau_y\rangle_f = \sin\theta \left(-\eta(a^*c + ac^*)\sin\phi - i(a^*c - ac^*)\cos\theta\cos\phi - n|c|^2\cos\beta\sin\theta + n|a|^2\sin\theta\cos(2\phi - \beta) \right), \quad (25)$$

$$\langle\tau_z\rangle_f = -2\eta|a|^2\cos\theta - \eta i(a^*c - ac^*)\sin\theta\cos(\beta - \phi) + n(a^*c + ac^*)\sin\theta\cos\theta\sin(\beta - \phi). \quad (26)$$

Experimentally, the CD-ARPES is an alternative method for probing the spin texture of topological surface states. The CD value is defined by taking the difference of photo-emission transition rate for photon with opposite helicity. The photo-emission transition rate are expressed as

$$\begin{aligned} I_\eta &\propto \sum_\sigma |\langle f_\sigma | \mathcal{A}_\eta \cdot \mathcal{P} | k \rangle|^2 \\ &= \frac{1}{4} (|a|^2 + |a|^2\cos^2\theta + 4|c|^2\sin^2\theta \\ &\quad + 2n\text{Im}[a^*c]\cos(\beta - \phi)\sin 2\theta \\ &\quad + 2n\eta\text{Re}[a^*c]\sin\theta\sin(\beta - \phi)), \end{aligned} \quad (27)$$

where Im and Re refers to the imaginary and real operators. The CD-ARPES spectra can thus be calculated as

$$\begin{aligned} I_{CD} &= \frac{I_R - I_L}{I_R + I_L} \\ &= 4n\text{Re}[a^*c]\sin\theta\sin(\beta - \phi) / \left(|a|^2(1 + \cos^2\theta) \right. \\ &\quad \left. + 4|c|^2\sin^2\theta + 2n\text{Im}[a^*c]\sin 2\theta\cos(\beta - \phi) \right). \end{aligned} \quad (28)$$

The calculated I_{CD} for Bi_2Se_3 (111) surface states are shown in Fig. 5.

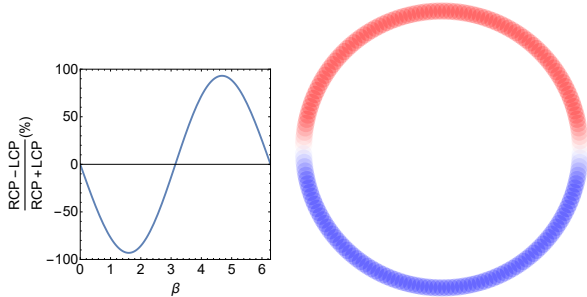


Figure 5. (Color online) The calculated CD-ARPES spectra for Bi_2Se_3 (111) surface states with $\theta = 3\pi/8$ and $\phi = 0$.

IV. SPIN-RESOLVED AND CD-ARPES FOR SMB_6 SURFACE STATES

Recently the mixed valence compound SmB_6 has been proposed to be a topological insulator and attracts lots of research interest¹⁶⁻²⁰. Unlike the Bi_2Se_3 family of materials, the strong correlation effects in mixed valence topological insulators are crucial in understanding electronic structure owing to the partially filled 4f bands. There are two main effects induced by the on-site Coulomb interaction among the 4f-electrons: the strong modification of the 4f band width and the correction to the effective spin orbit coupling and crystal field. As a consequence, the band inversion in the modified band structure happens between 5d and 4f band around three X points at the BZ boundary. If a surface terminated in the (001) direction, one X point projects to the $\bar{\Gamma}$ points on the surface BZ and the other two X points project to \bar{Y} and \bar{X} points and leading to three different Dirac points on the (001) surfaces. In this section, we will discuss the relations between the above mentioned three spin textures and calculate the CD spectrum for the surface states near $\bar{\Gamma}$, \bar{Y} and \bar{X} points.

A. Surface states at $\bar{\Gamma}$ point

The crystalline symmetry at $\bar{\Gamma}$ point is characterized by double group of C_{4v} . From group theory we know that there are two kinds of two-dimensional irreducible representations for the double group of C_{4v} , which are $j_z = \pm 1/2$ and $j_z = \pm 3/2$ representation respectively. The first-principles calculations show that the Dirac surface states at $\bar{\Gamma}$ point belong to the representation of $j_z = \pm 3/2$. Therefore the effective Hamiltonian for surface states near $\bar{\Gamma}$ point is given as^{21,22}

$$H_{\bar{\Gamma}} = -\hbar v(k_y\sigma_x + k_x\sigma_y) = -\hbar v k(\sin\beta\sigma_x + \cos\beta\sigma_y) \quad (29)$$

in the basis of $\{|j_z = +\frac{3}{2}\rangle, |j_z = -\frac{3}{2}\rangle\}$, where β is the angle between \mathbf{k} and the $+k_x$ direction and $\sigma_{x,y}$ are the Pauli matrices in the pseudo spin space expand by $|j_z = \pm\frac{3}{2}\rangle$.

The eigenvalue and Bloch periodic eigenstate near $\bar{\Gamma}$ point are $E_n = n\hbar v k$ and

$$|\mathbf{k}\rangle_n = \frac{1}{\sqrt{2}} \left(n i e^{i\beta} |+\frac{3}{2}\rangle_i + |-\frac{3}{2}\rangle_i \right) = \frac{1}{\sqrt{2}} \begin{bmatrix} i n e^{i\beta} \\ 1 \end{bmatrix}. \quad (30)$$

The pseudo spin texture are calculated as

$$\langle\boldsymbol{\sigma}\rangle_{\mathbf{k},n} \propto -n(\sin\beta, \cos\beta, 0). \quad (31)$$

The “g-factor” connecting real spin operator \mathbf{s} and pseudo spin operator $\boldsymbol{\sigma}$ in Eq. (3) are given as²² $g_{xx} = 0.095$, $g_{yy} = -0.095$, $g_{zz} = 0.068$. Then the real spin vectors for the TSS are given by

$$\langle\mathbf{s}\rangle_{\mathbf{k},n} \propto -n(g_{xx}\sin\beta, g_{yy}\cos\beta, 0) \quad (32)$$

as shown in Fig. 6.

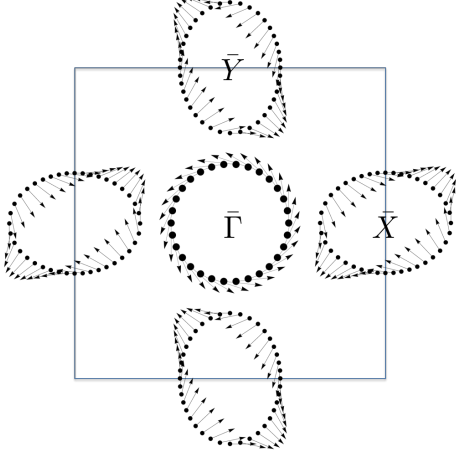


Figure 6. Real spin texture of the SmB_6 (001) surface states near $\bar{\Gamma}$, \bar{Y} and \bar{X} point with energy above the Dirac cone.

The C_{4v} symmetry contains C_4 rotation symmetry and mirror symmetry M_x . The basis function $|\pm \frac{3}{2}\rangle_i$ for initial states and $|\pm \frac{1}{2}\rangle_f$ for final states satisfy the following symmetry properties

$$M_x |\pm \frac{3}{2}\rangle_i = -i |\mp \frac{3}{2}\rangle_i, \quad (33)$$

$$C_4 |\pm \frac{3}{2}\rangle_i = e^{-i\frac{2\pi}{4} \times (\pm \frac{3}{2})} |\pm \frac{3}{2}\rangle_i, \quad (34)$$

$$C_4 |\pm \frac{1}{2}\rangle_f = e^{-i\frac{2\pi}{4} \times (\pm \frac{1}{2})} |\pm \frac{1}{2}\rangle_f. \quad (35)$$

With the similar arguments used in the previous section, the nonzero matrix elements in Eq. (7) are obtained as listed below

$${}_f\langle +\frac{1}{2} | \mathcal{P}_- | +\frac{3}{2}\rangle_i = {}_f\langle -\frac{1}{2} | \mathcal{P}_+ | -\frac{3}{2}\rangle_i = a. \quad (36)$$

The matrix element for \mathcal{P}_z is vanish for that it cannot conserve the total angular momentum along z direction. This results is different from the Bi_2Se_3 case, where the surface states with $j_z = \pm \frac{1}{2}$ lead to the nonzero matrix element for \mathcal{P}_z as shown in Eq. (17). Substitute Eq. (30) and Eq. (36) into Eq. (7), the final state is obtained as

$$|f\rangle \propto \frac{a}{\sqrt{2}} \begin{bmatrix} ine^{i\beta} \mathcal{A}_+ \\ \mathcal{A}_- \end{bmatrix}. \quad (37)$$

(i) For σ -polarized light, $\mathcal{A}_\sigma = A_0(-\sin\phi, \cos\phi, 0)$, the final states takes the form of

$$|f\rangle \propto \frac{aA_0}{\sqrt{2}} \begin{bmatrix} -ine^{i(\beta+2\phi)} \\ 1 \end{bmatrix}, \quad (38)$$

and the spin polarization for photo-electrons can be calculated as

$$\langle \tau \rangle_f \propto n [\sin(\beta + 2\phi), \cos(\beta + 2\phi), 0] \quad (39)$$

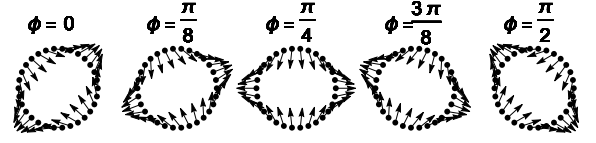


Figure 7. Spin polarization of photon-electrons with σ -polarized light. Arrows indicate the spin component in the xy plane.

as shown in Fig. 7. The spin texture takes a different rotation manner as tuning ϕ from $\phi = 0$ to $\pi/2$ compare to Bi_2Se_3 as shown in Fig. 3.

(ii) For π -polarized light, $\mathcal{A}_\pi = A_0(\cos\theta\cos\phi, \cos\theta\sin\phi, -\sin\theta)$, the final states can be calculated as

$$|f\rangle \propto \frac{aA_0\cos\theta}{\sqrt{2}} \begin{bmatrix} ine^{i(\beta+2\phi)} \\ 1 \end{bmatrix}, \quad (40)$$

and the spin vector for $|f\rangle$ is calculated as

$$\langle \tau \rangle_f \propto -n\cos^2\theta(\sin(\beta + 2\phi), \cos(\beta + 2\phi), 0) \quad (41)$$

as shown in Fig. 8. Different to the case in Bi_2Se_3 system, for SmB_6 (001) surface states the π -polarized light does not induce the z direction component in the spin orientation, for the photo-emission matrix element of \mathcal{P}_z is vanish under the symmetry constraint.

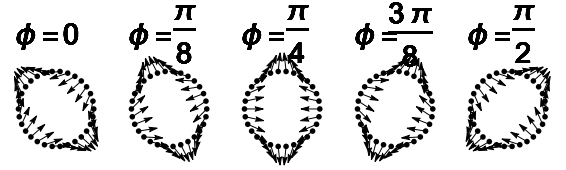


Figure 8. Spin polarization of photon-electrons with π -polarized light. Arrows indicate the spin component in the xy plane.

(iii) For circular polarized light, $\mathcal{A}_\eta = A_0(\cos\theta\cos\phi + i\eta\sin\phi, \cos\theta\sin\phi - i\eta\cos\phi, -\sin\theta)$, where $\eta = \pm 1$ indicate the RCP/LCP light, the final states can be calculated as

$$|f\rangle \propto \frac{aA_0}{\sqrt{2}} \begin{bmatrix} -in(\cos\theta + \eta)e^{i(\beta+2\phi)} \\ (\cos\theta - \eta) \end{bmatrix} \quad (42)$$

with spin vector

$$\langle \tau \rangle_f \propto (n\sin^2\theta\sin(\beta + 2\phi), n\sin^2\theta\cos(\beta + 2\phi), 2\eta\cos\theta) \quad (43)$$

The photo-emission transition rate is calculated as

$$I_\eta = \frac{|a|^2}{4}(1 + \cos^2\theta), \quad (44)$$

which is independent with light helicity η and lead to $I_{CD} = 0$. The reason for obtained the vanish CD spectra

is that here we only keep up to the zeroth order perturbation for the initial states. Keep up to the first order perturbations terms in the initial states, we get²³

$$|\phi_{\pm}\rangle = a_1|\pm\frac{3}{2}\rangle \pm ia_2k_{\pm}|\pm\frac{1}{2}\rangle \pm ia_3k_{\mp}|\pm\frac{5}{2}\rangle, \quad (45)$$

where $a_{1,2,3}$ are material dependent parameters. The above wave functions are constructed by considering the conservation of the total angular momentum j_z in z direction²³. For example, k_{\pm} carry the angular momentum ± 1 , so the total angular momentum in z direction is $\pm 1/2$ for the second and third terms in Eq. (45).

Taking the symmetry consideration into the matrix elements of \mathcal{P} , we find that the following terms are nonzero

$$f\langle+\frac{1}{2}|\mathcal{P}_+|-\frac{1}{2}\rangle_i = f\langle-\frac{1}{2}|\mathcal{P}_-|+\frac{1}{2}\rangle_i = c_1, \quad (46)$$

$$f\langle+\frac{1}{2}|\mathcal{P}_-|+\frac{3}{2}\rangle_i = f\langle-\frac{1}{2}|\mathcal{P}_+|-\frac{3}{2}\rangle_i = c_2, \quad (47)$$

$$f\langle+\frac{1}{2}|\mathcal{P}_-|-\frac{5}{2}\rangle_i = f\langle-\frac{1}{2}|\mathcal{P}_+|+\frac{5}{2}\rangle_i = c_3, \quad (48)$$

$$f\langle+\frac{1}{2}|\mathcal{P}_z|+\frac{1}{2}\rangle_i = f\langle-\frac{1}{2}|\mathcal{P}_z|-\frac{1}{2}\rangle_i = c_4. \quad (49)$$

The difference of photo-emission transition rate under right- and left-handed circular polarized light is calculated as

$$I_R - I_L = \left[\text{Im}[c_4c_1^*]a_2nk\cos(3\beta + \phi) + (\text{Im}[c_4c_2^*]a_1 + \text{Im}[c_3c_4^*]a_3nk)\cos(\beta - \phi) \right] 2a_2k\sin\theta, \quad (50)$$

and the CD values around $\bar{\Gamma}$ point are shown in Fig. 9 with parameters $a_1 = -0.25$, $a_2 = 0.6$, $a_3 = -0.52$, $c_1 = -0.2 - 0.1i$, $c_2 = -0.6 + 0.1i$, $c_3 = -0.6 - 0.4i$, $c_4 = 0.1 - 0.3i$ where c_i with unit $\text{\AA} \cdot \text{m}$ and these parameters qualitatively reproduce the experimental result in Ref. 24.

B. Surface states at \bar{Y} point

The symmetry of Dirac type surface states locate at \bar{Y} and \bar{X} points are characterized by C_{2v} and time reversal symmetry. The first-principles calculations show that the eigenstates possess angular momentum $j_z = \pm\frac{3}{2}$ at these surface Dirac points. The surface states Hamiltonian at \bar{Y} point is given as²²

$$H_{\bar{Y}} = ak_y\sigma_x + bk_x\sigma_y \quad (51)$$

in basis of $\{|j_z = +3/2\rangle, |j_z = -3/2\rangle\}$, where the Pauli matrices indicate the pseudo spin space, $\sigma_{\pm} = \sigma_x \pm i\sigma_y$, a, b are material dependent parameters. The eigenvalues

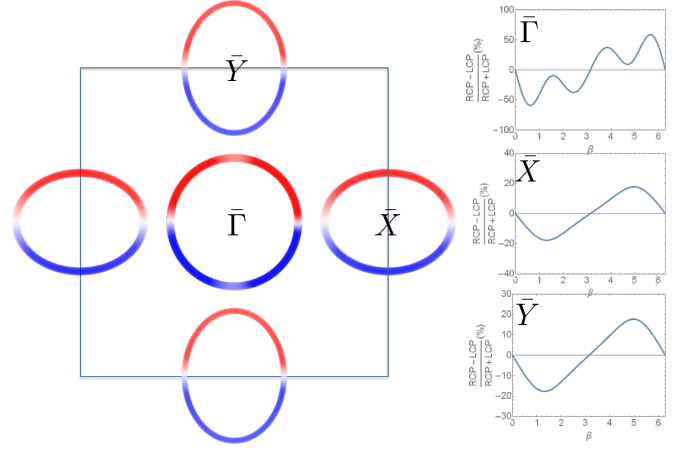


Figure 9. (Color online) Calculated CD spectra for SmB_6 (001) surface states near $\bar{\Gamma}$, \bar{Y} and \bar{X} points.

and Bloch periodic eigenstates are $E_n = n\sqrt{a^2k_y^2 + b^2k_x^2}$ and

$$|k\rangle_n = \frac{1}{\sqrt{2}\sqrt{a^2k_y^2 + b^2k_x^2}} \begin{bmatrix} n\sqrt{a^2k_y^2 + b^2k_x^2} \\ ak_y + ibk_x \end{bmatrix}. \quad (52)$$

The pseudo spin texture are calculated as

$$\langle\sigma\rangle_n \propto n(ak_y, bk_x, 0). \quad (53)$$

The relation between real spin and pseudo spin are $\langle s_x, s_y, s_z \rangle = \langle g_{xx}\sigma_x, g_{yy}\sigma_y, g_{zz}\sigma_z \rangle$, with $g_{xx} = 0.0687$, $g_{yy} = -0.1223$, $g_{zz} = -0.1484$. Then the real spin texture are calculated as

$$\langle s \rangle_{\mathbf{k},n} \propto n(ag_{xx}k_y, bg_{yy}k_x, 0), \quad (54)$$

as shown in Fig. 6 with parameters $a = -0.04$, $b = 0.05$.

The nonzero matrix elements in Eq. (7) has the following relations under C_{2v} symmetry constraint

$$f\langle+\frac{1}{2}|\mathcal{P}_+|+\frac{3}{2}\rangle_i = f\langle-\frac{1}{2}|\mathcal{P}_-|-\frac{3}{2}\rangle_i = p, \quad (55)$$

$$f\langle+\frac{1}{2}|\mathcal{P}_-|+\frac{3}{2}\rangle_i = f\langle-\frac{1}{2}|\mathcal{P}_+|-\frac{3}{2}\rangle_i = q. \quad (56)$$

Then the final states in Eq. (7) can be written as

$$|f\rangle = \frac{1}{\sqrt{2(a^2k_y^2 + b^2k_x^2)}} \begin{bmatrix} n\sqrt{a^2k_y^2 + b^2k_x^2}(q\mathcal{A}_+ + p\mathcal{A}_-) \\ (ak_y + ibk_x)(p\mathcal{A}_+ + q\mathcal{A}_-) \end{bmatrix} \quad (57)$$

With this formula, the spin polarization of photon-emitted electron can be easily calculated as discussed before.

(i) For σ -polarized light, the spin vector of the photo-

emitted electrons is given as

$$\langle \tau_x \rangle_f = n \left[ak_y((p^*q + pq^*) - \cos 2\phi(|p|^2 + |q|^2)) + bk_x \sin 2\phi(|p|^2 - |q|^2) \right] / \sqrt{a^2 k_y^2 + b^2 k_x^2}, \quad (58)$$

$$\langle \tau_y \rangle_f = n \left[bk_x((p^*q + pq^*) - \cos 2\phi(|p|^2 + |q|^2)) + ak_{xy} \sin 2\phi(|q|^2 - |p|^2) \right] / \sqrt{a^2 k_y^2 + b^2 k_x^2}, \quad (59)$$

$$\langle \tau_z \rangle_f = -i(p^*q - pq^*) \sin 2\phi. \quad (60)$$

The spin texture is shown in Fig. 10 with parameters $p = 0.16 - 0.1i$ and $q = -0.5 + 0.1i$ with unit $\text{Å} \cdot \text{m}$.

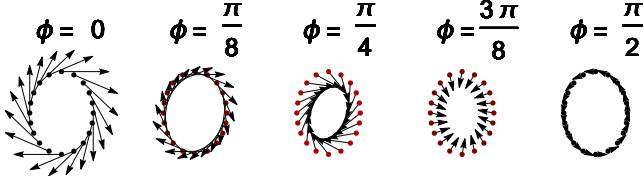


Figure 10. (Color online) Spin polarization of photon-electrons with σ -polarized light. Arrows indicate the spin component in the xy plane. Color indicate the spin z component: red for $\langle \tau_z \rangle < 0$, blue for $\langle \tau_z \rangle > 0$ and black for $\langle \tau_z \rangle = 0$.

(ii) For π -polarized light, the spin vectors are

$$\langle \tau_x \rangle_f = n \cos^2 \theta \left[ak_y(p^*q + pq^* + \cos 2\phi(|p|^2 + |q|^2)) - bk_x \sin 2\phi(|p|^2 - |q|^2) \right] / \sqrt{a^2 k_y^2 + b^2 k_x^2}, \quad (61)$$

$$\langle \tau_y \rangle_f = n \cos^2 \theta \left[bk_x(p^*q + pq^* + \cos 2\phi(|p|^2 + |q|^2)) - ak_y \sin 2\phi(|q|^2 - |p|^2) \right] / \sqrt{a^2 k_y^2 + b^2 k_x^2}, \quad (62)$$

$$\langle \tau_z \rangle_f = i \cos^2 \theta (p^*q - pq^*) \sin 2\phi. \quad (63)$$

The spin texture is shown in Fig. 11.

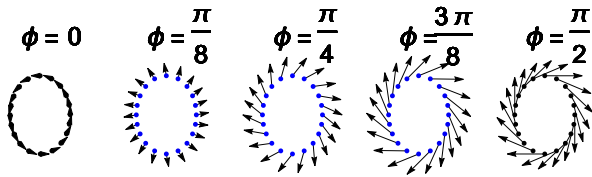


Figure 11. (Color online) Spin polarization of photon-electrons with π -polarized light. Arrows indicate the spin component in the xy plane. Color indicate the spin z component: red for $\langle \tau_z \rangle < 0$, blue for $\langle \tau_z \rangle > 0$ and black for $\langle \tau_z \rangle = 0$.

(iii) For the RCP/LCP light, the nonzero CD spectrum can be obtained by considering the high order perturba-

tions in the wave function as shown in Eq. (45). Keeping the nonzero matrix elements listed below

$$\langle +\frac{1}{2} | \mathcal{P}_+ | -\frac{1}{2} \rangle = \langle -\frac{1}{2} | \mathcal{P}_- | +\frac{1}{2} \rangle = d_1,$$

$$\langle +\frac{1}{2} | \mathcal{P}_+ | +\frac{3}{2} \rangle = \langle -\frac{1}{2} | \mathcal{P}_- | -\frac{3}{2} \rangle = d_2,$$

$$\langle +\frac{1}{2} | \mathcal{P}_+ | -\frac{5}{2} \rangle = \langle -\frac{1}{2} | \mathcal{P}_- | +\frac{5}{2} \rangle = d_3,$$

$$\langle +\frac{1}{2} | \mathcal{P}_- | -\frac{1}{2} \rangle = \langle -\frac{1}{2} | \mathcal{P}_+ | +\frac{1}{2} \rangle = d_4,$$

$$\langle +\frac{1}{2} | \mathcal{P}_- | +\frac{3}{2} \rangle = \langle -\frac{1}{2} | \mathcal{P}_+ | -\frac{3}{2} \rangle = d_5,$$

$$\langle +\frac{1}{2} | \mathcal{P}_- | -\frac{5}{2} \rangle = \langle -\frac{1}{2} | \mathcal{P}_+ | +\frac{5}{2} \rangle = d_6,$$

$$\langle +\frac{1}{2} | \mathcal{P}_z | +\frac{1}{2} \rangle = \langle -\frac{1}{2} | \mathcal{P}_z | -\frac{1}{2} \rangle = d_7,$$

$$\langle +\frac{1}{2} | \mathcal{P}_z | -\frac{3}{2} \rangle = \langle -\frac{1}{2} | \mathcal{P}_z | +\frac{3}{2} \rangle = d_8,$$

$$\langle +\frac{1}{2} | \mathcal{P}_z | +\frac{5}{2} \rangle = \langle -\frac{1}{2} | \mathcal{P}_z | -\frac{5}{2} \rangle = d_9, \quad (64)$$

the CD values can be obtained by using Eq. (7), Eq. (27) and Eq. (28). The expressions for the CD values around \bar{Y} and \bar{X} point are very lengthy and will not be given here. We only show the numerical results in Fig. 9 with parameters $a_1 = -0.2$, $a_2 = 0.7$, $a_3 = 0.42$, $d_1 = (-0.1 + 0.1i)$, $d_5 = (-0.5 + 0.1i)$, $d_6 = (-0.02 + 0.04i)$, $d_7 = (0.2 - 0.3i)$, $d_2 = (0.16 - 0.1i)$, $d_3 = (0.06 - 0.02i)$, $d_4 = (0.1 - 0.05i)$, $d_8 = (0.06 - 0.02i)$ and $d_9 = (0.01 - 0.03i)$ where d_i with unit $\text{Å} \cdot \text{m}$. These parameters well reproduce the experimental result in Ref. 24.

V. CONCLUSION

To summarize, we discussed three different definition of the spin texture for the topological surface states, namely the pseudo spin and real spin orientation for electronic states inside the crystal and that of the photo-emitted electrons in the vacuum. Taking Bi_2Se_3 and SmB_6 as examples, we revealed that the above three spin textures are different and should be clarified rigorously and studied separately. By considering the symmetry properties of the photo-emission matrix element, we calculated the spin polarization and CD spectrum of the photo-electrons

for these two compounds which can be observed in the spin-resolved and CD ARPES experiment.

Acknowledgments — This work was supported by the National Natural Science Foundation of China, the 973 program of China (No.2013CB921700), and the “Strategic Priority Research Program (B)” of the Chinese Academy of Sciences (No.XDB07020100). R.Y. acknowledges funding from the Fundamental Research Funds for the Central Universities (Grant No.AUGA5710059415).

Appendix A: Some discussions about vector \mathbf{A}

As shown in Fig. 1 the local coordinate system $x'y'z'$ and the global coordinate system xyz are related by

$$x' = (\cos\theta\cos\phi, \cos\theta\sin\phi, -\sin\theta), \quad (\text{A1})$$

$$y' = (-\sin\phi, \cos\phi, 0), \quad (\text{A2})$$

$$z' = (\sin\theta\cos\phi, \sin\theta\sin\phi, \cos\theta). \quad (\text{A3})$$

For π -polarized light, the vector \mathbf{A} are expressed as

$$\mathbf{A}'_{\pi} = (A_0\cos\omega t, 0, 0) \xrightarrow{F.T.} (A_0, 0, 0), \quad (\text{A4})$$

in the local coordinate system and

$$\mathbf{A}_{\pi} = A_0(\cos\theta\cos\phi, \cos\theta\sin\phi, -\sin\theta). \quad (\text{A5})$$

in the global coordinate system.

For σ -polarized light, we have

$$\mathbf{A}'_{\sigma} = (0, A_0\cos\omega t, 0) \xrightarrow{F.T.} (0, A_0, 0), \quad (\text{A6})$$

in the local coordinate system and

$$\mathbf{A}_{\sigma} = A_0(-\sin\phi, \cos\phi, 0), \quad (\text{A7})$$

in the global coordinate system.

For left and right circular polarized light we get

$$\mathbf{A}'_{\eta} = A_0(\cos\omega t, \eta \sin\omega t, 0) \xrightarrow{F.T.} A_0(1, -\eta i, 0), \quad (\text{A8})$$

in the local coordinate system, where $\eta = \pm 1$ indicate the right and left circular polarized light. In the global coordinate system \mathbf{A} has the following form:

$$\mathbf{A}_{\eta} = A_0(\cos\theta\cos\phi + \eta i\sin\phi, \cos\theta\sin\phi - \eta i\cos\phi, -\sin\theta). \quad (\text{A9})$$

-
- * daix@iphy.ac.cn
- ¹ M. Z. Hasan and C. L. Kane, *Rev. Mod. Phys.* **82**, 3045 (2010).
 - ² X.-L. Qi and S.-C. Zhang, *Rev. Mod. Phys.* **83**, 1057 (2011).
 - ³ J. W. McIver, D. Hsieh, H. Steinberg, P. Jarillo-Herrero, and N. Gedik, *Nature Nanotechnology* **7**, 96 (2011).
 - ⁴ Y. H. Wang, D. Hsieh, D. Pilon, L. Fu, D. R. Gardner, Y. S. Lee, and N. Gedik, *Phys. Rev. Lett.* **107**, 207602 (2011).
 - ⁵ C.-H. Park and S. G. Louie, *Phys. Rev. Lett.* **109**, 097601 (2012).
 - ⁶ C. Jozwiak, C.-H. Park, K. Gotlieb, C. Hwang, D.-H. Lee, S. G. Louie, J. D. Denlinger, C. R. Rotundu, R. J. Birge-neau, Z. Hussain, and A. Lanzara, *Nature Physics* **9**, 293 (2013).
 - ⁷ S. R. Park, J. Han, C. Kim, Y. Y. Koh, C. Kim, H. Lee, H. J. Choi, J. H. Han, K. D. Lee, N. J. Hur, M. Arita, K. Shimada, H. Namatame, and M. Taniguchi, *Phys. Rev. Lett.* **108**, 046805 (2012).
 - ⁸ Y. Wang and N. Gedik, *physica status solidi (RRL) - Rapid Research Letters* **7**, 64 (2013).
 - ⁹ J. Sánchez-Barriga, A. Varykhalov, J. Braun, S.-Y. Xu, N. Alidoust, O. Kornilov, J. Minár, K. Hummer, G. Springholz, G. Bauer, R. Schumann, L. V. Yashina, H. Ebert, M. Z. Hasan, and O. Rader, *Phys. Rev. X* **4**, 011046 (2014).
 - ¹⁰ Z.-H. Zhu, C. N. Veenstra, S. Zhdanovich, M. P. Schneider, T. Okuda, K. Miyamoto, S.-Y. Zhu, H. Namatame, M. Taniguchi, M. W. Haverkort, I. S. Elfimov, and A. Damascelli, *Phys. Rev. Lett.* **112**, 076802 (2014).
 - ¹¹ C.-X. Liu, X.-L. Qi, H. Zhang, X. Dai, Z. Fang, and S.-C. Zhang, *Phys. Rev. B* **82**, 045122 (2010).
 - ¹² H. Zhang, C.-X. Liu, X. L. Qi, X. Dai, Z. Fang, and S.-C. Zhang, *Nature Physics* **5**, 438 (2009).
 - ¹³ Y. Xia, D. Qian, D. Hsieh, L. Wray, A. Pal, H. Lin, A. Bansil, D. Grauer, Y. S. Hor, R. J. Cava, and M. Z. Hasan, *Nature Physics* **5**, 398 (2009).
 - ¹⁴ Z. Alpichshev, J. G. Analytis, J.-H. Chu, I. R. Fisher, Y. L. Chen, Z. X. Shen, A. Fang, and A. Kapitulnik, *Phys. Rev. Lett.* **104**, 016401 (2010).
 - ¹⁵ H. Beidenkopf, P. Roushan, J. Seo, L. Gorman, I. Drozdov, Y. S. Hor, R. J. Cava, and A. Yazdani, *Nature Physics* **7**, 939 (2011).
 - ¹⁶ M. Dzero, K. Sun, V. Galitski, and P. Coleman, *Phys. Rev. Lett.* **104**, 106408 (2010).
 - ¹⁷ M. Dzero, K. Sun, P. Coleman, and V. Galitski, *Phys. Rev. B* **85**, 045130 (2012).
 - ¹⁸ F. Lu, J. Zhao, H. Weng, Z. Fang, and X. Dai, *Phys. Rev. Lett.* **110**, 096401 (2013).
 - ¹⁹ V. Alexandrov, M. Dzero, and P. Coleman, *Phys. Rev. Lett.* **111**, 226403 (2013).
 - ²⁰ M. Dzero and V. Galitski, *Journal of Experimental and Theoretical Physics* **117**, 499 (2013).
 - ²¹ B. Roy, J. D. Sau, M. Dzero, and V. Galitski, *Phys. Rev. B* **90**, 155314 (2014).
 - ²² R. Yu, H. Weng, X. Hu, Z. Fang, and X. Dai, *New Journal of Physics* **17**, 023012 (2015).
 - ²³ H. Zhang, C.-X. Liu, and S.-C. Zhang, *Phys. Rev. Lett.* **111**, 066801 (2013).

²⁴ J. Jiang, S. Li, T. Zhang, Z. Sun, F. Chen, Z. R. Ye, M. Xu, Q. Q. Ge, S. Y. Tan, X. H. Niu, M. Xia, B. P. Xie, Y. F.

Li, X. H. Chen, H. H. Wen, and D. L. Feng, *Nature Communications* **4**, 3010 (2013).